ELSEVIER

Journal of Alloys and Compounds 434–435 (2007) 252–254

Journal of ALLOYS AND COMPOUNDS

www.elsevier.com/locate/jallcom

Synthesis routes for controlling the microstructure in nanostructured $Al_{88}Y_7Fe_5$ alloys

N. Boucharat [a,*], R. Hebert [a], H. Rösner [a], R.Z. Valiev [b], G. Wilde [a,**]

[a] *Forschungszentrum Karlsruhe, Institute of Nanotechnology, P.O. Box 3640, 76021 Karlsruhe, Germany*
[b] *Institute of Physics of Advanced Materials, Ufa State Aviation Technical University, 450 000 Ufa, Russia*

Available online 29 September 2006

Abstract

Deformation-induced nanocrystallization has been investigated in metallic $Al_{88}Y_7Fe_5$ glasses. In situ TEM tensile tests at room temperature give new evidence to the atomic mobility enhancement as the underlying mechanism of nanocrystallization in shear-bands that form during deformation. High pressure torsion straining allows to control the microstructure in producing homogeneous bulk nanostructures at an extremely high number density of nanocrystals.

Keywords: Amorphous metals; Nanostructures; Liquid quenching; Strain; High pressure

1. Introduction

The common way to produce nanostructures from marginally glass forming alloys is to apply low temperature isothermal treatments [1]. As reported earlier [2], number densities of Al-nanocrystals as high as 10^{21} m^{-3} have been reached in as-spun $Al_{88}Y_7Fe_5$ alloy initially amorphous after short time annealing at 245 °C, i.e. about 30 °C below the onset temperature of the glass transition. However, nanocrystallization reactions during deformation of metallic glasses at room temperature have been observed for different deformation modes such as bending [3,4], ball-milling [5] nanoindentation [6] or cold-rolling (CR) [7]. Deformation of metallic glasses at room temperature is dominated by the formation of shear-bands, where nanocrystals preferentially develop. However, deformation-induced nanocrystallization has caused controversial discussions as to the underlying mechanisms that induce the nanocrystal formation. With the new evidence that nanocrystals might not only be confined to shear-bands [7], it seems that severe plastic deformation processing (SPD) could serve as a new synthesis route for controlling the microstructure, especially to produce nanostructured materials with an extremely high number density of homogeneously distributed nanocrystals [8]. To examine the effect of plastic deformation on the crystallization reaction and thus on the resulting microstructure, structural analyses of glassy $Al_{88}Y_7Fe_5$ alloys have been performed during and after in situ TEM tensile testing or high-pressure torsion straining (HPT) at room temperature.

2. Nanocrystallization described as an athermal process

Related to deformation-induced nanocrystallization, hypotheses have been advanced to account for the underlying mechanism. It has been suggested that the formation of crystallites is caused by either a local adiabatic heating during the formation of shear-bands [9] or, alternatively, by an increase of the atomic mobility in the shear-bands due to an increased free volume [6]. In order to rationalize deformation-induced nanocrystallization reactions at room temperature, in situ TEM (Philips, Tecnai F20 ST) tensile testing has been performed with a rapidly quenched $Al_{88}Y_7Fe_5$ ribbon using a Gatan single-tilt stage. The HRTEM micrograph in Fig. 1a indicates that shear-bands formed during the tensile straining, but they do not contain nanocrystals. After exposing the sample to the electron beam, nanocrystals develop within shear-bands (Fig. 1b), whereas the amorphous matrix remains free from crystallites after an identical treatment. Recent TEM examinations of a cold-rolled $Al_{88}Y_7Fe_5$ alloy support this observation [7]. It has been shown by microcalorimetry analyses that Al-nanocrystals

* Corresponding author. Tel.: +49 7247 82 6450; fax: +49 7247 82 6368.
** Corresponding author. Tel.: +49 7247 82 6414; fax: +49 7247 82 6368.
E-mail addresses: nancy.boucharat@int.fzk.de (N. Boucharat), Gerd.wilde@int.fzk.de (G. Wilde).

0925-8388/$ – see front matter © 2006 Elsevier B.V. All rights reserved.
doi:10.1016/j.jallcom.2006.08.128

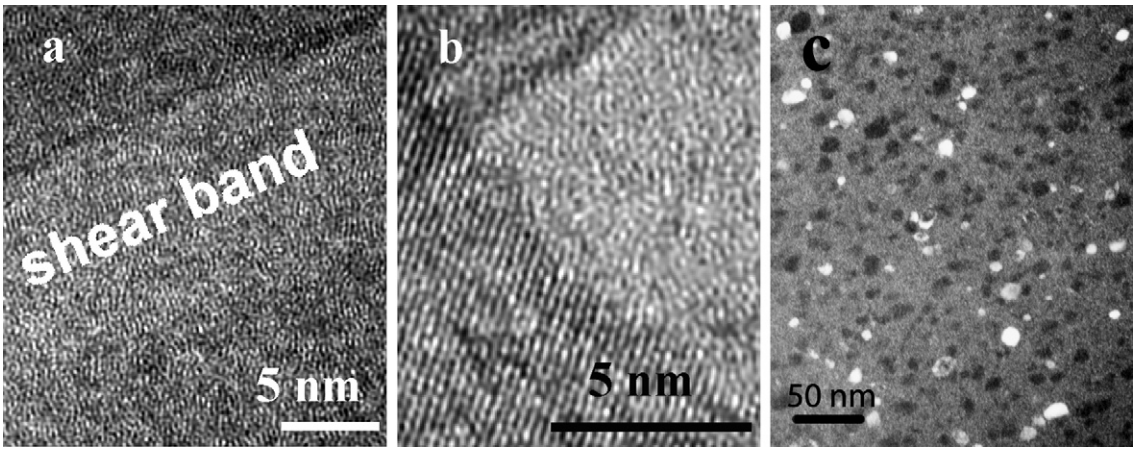

Fig. 1. TEM analyses of a glassy $Al_{88}Y_7Fe_5$ ribbon: (a) HRTEM micrograph showing a shear-band that formed during the deformation. (b) HRTEM micrograph of the shear-band region after exposure to the electron beam. Al-nanocrystals develop as indicated by the presence of lattice fringes. (c) Dark-field image of a HPT sample showing that an extremely high number density of Al-nanocrystals develops under large shear strains.

slowly develop in deformed samples within the shears-bands at temperature as low as 60 °C, whereas as-spun samples during identical microcalorimetry measurements remain free from crystallites. These results provide additional experimental evidence that the nanocrystals develop predominantly within the shear-bands due to an enhancement of the atomic mobility thus promoting the nanocrystal growth. However, nanocrystals outside the shear-bands were recently observed in samples processed by CR [7] indicating that the amorphous matrix is also affected by plastic deformation. This additional observation indicates that plastic deformation at large strain could be applied to produce homogeneous bulk nanostructured materials of marginally glass forming systems.

3. SPD-induced nanocrystallization

In order to investigate the effect of large strains on the microstructure at the nanometer level, disks were prepared with a diameter of 8 mm and a thickness of 0.17 ± 0.02 mm by high pressure torsion straining at room temperature from $Al_{88}Y_7Fe_5$ glassy ribbons. The shear deformation was realized by subjecting the ribbons to five whole turns at a speed of $0.017\ s^{-1}$ under a high compressive pressure of 6 GPa. The equivalent strain was estimated at $\varepsilon = 144$ which is considerably higher than equivalent strains usually obtained by other modes of deformation. As illustrated in the dark-field TEM image (TEM, Philips CM 30) in Fig. 1c, Al-nanocrystals develop homogeneously within the amorphous matrix, whereas as-spun ribbons do not show any signal of crystallinity. The average particle size was about 12 nm, which is smaller than typical particle sizes obtained by low temperature isothermal treatments [2,10]. The number density of Al-nanocrystals has been estimated by counting particles on a dark-field TEM image. The sample thickness of the respective sample region was determined by the log-ratio of the integral intensities of the plasmon peaks and the zero loss peak of electron energy loss spectroscopy spectra (EELS). The obtained number density amounts to about $10^{22}\ m^{-3}$. This has to be regarded as a lower limit since some nanocrystals have certainly been omitted from counting due to low contrast conditions or particle overlap. The results show clearly that the increase of the nanocrystal number density after SPD processing is remarkable, since values of $3–4.8 \times 10^{21}\ m^{-3}$ and 1.0×10^{21} have been obtained after annealing at 245 °C [2] or after CR to an equivalent strain of $\varepsilon = -11.5$ [11], respectively. From the examinations reported for deformation at moderate strains [7], the homogeneous dispersion of nanocrystals is linked to either the formation of an extremely high density of shear-bands, or the modification of the amorphous matrix such that nanocrystal formation in the volume is favored even at ambient temperature. Additional processes such as the fragmentation of the particles could also account for the increase of the nanocrystal number density and for the retention of very small particles [7].

4. Combined processes for tuning the microstructure

Beyond serving as a consolidation process that allows producing homogeneous nanostructured bulk materials from

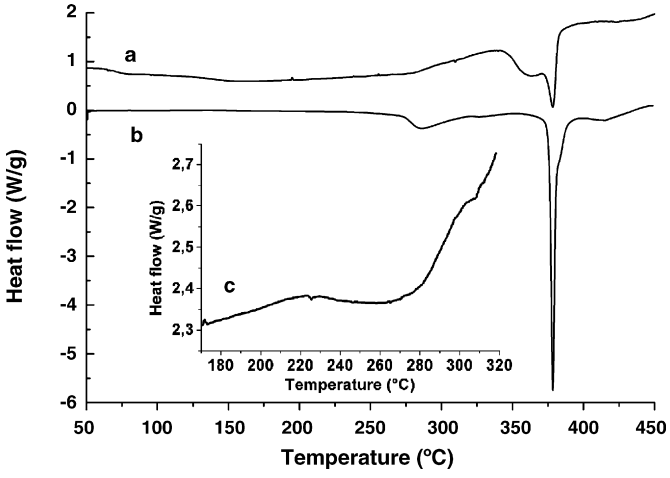

Fig. 2. Continuous DSC traces at 20 °C min^{-1} of $Al_{88}Y_7Fe_5$: (a) disks prepared by HPT processing; (b) As-spun sample; (c) HPT sample after cycling up to 200 °C. The signal shows a small exothermic peak at an onset temperature of about 220 °C that is attributed to the primary crystallization reaction.

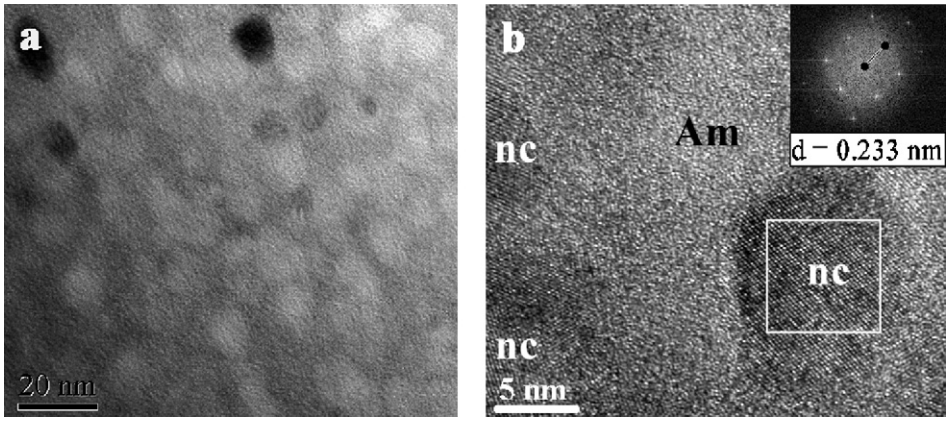

Fig. 3. TEM analyses of a HPT $Al_{88}Y_7Fe_5$ disk that has been held at 245 °C for 148 h: (a) bright-field image indicating the presence of a high number density of nanocrystals. (b) The HRTEM micrograph shows that nanocrystals (nc) are surrounded by an amorphous phase (Am). An interplanar spacing value of 0.233 nm is obtained from the FFT pattern of a nanocrystal (highlighted by the rectangular frame) that corresponds to {1 1 1} lattice planes of fcc-Al (inset).

rapidly quenched ribbons, a great interest exists in SPD processing for developing ways to produce completely nanocrystalline materials. One promising synthesis route is presented by a combination of SPD and subsequent thermal treatments to induce the crystallization of the remaining amorphous matrix. For this purpose, annealing at 245 °C for 148 h was performed. This temperature was chosen in agreement with the thermal behavior of the deformed samples (Fig. 2a). Unlike as-spun samples (Fig. 2b), the DSC trace of HPT samples does not show a clear primary crystallization peak. Instead, a small decrease of the heat flow occurs at temperatures below 200 °C that is attributed to strain relaxation and Al-nanocrystal growth in the shear-bands at low temperatures [7]. After cycling the sample up to 200 °C, a weak exothermic signal starting at about 220 °C is detectable (Fig. 2c) upon subsequent heating, which is related to further nanocrystal development. The signal appears at about 50 °C below the onset temperature of the primary crystallization of as-spun $Al_{88}Y_7Fe_5$ (Fig. 2b) supplying new indications that strain can also induce structural instabilities of the amorphous state, leading to early crystallization. Hence, the low annealing temperature of 245 °C is expected to limit the particle growth, but should be sufficiently high to induce the crystallization of the remaining amorphous matrix. The bright-field TEM micrograph obtained on a thin region of the TEM foil reveals clearly crystallites with a size of about 10 nm (Fig. 3a). However, the sample is partially crystallized as observed on the HRTEM image in Fig. 3b, that shows nanocrystals surrounded by an amorphous phase. The interplanar spacing value of 0.233 nm obtained from the FFT pattern of a crystallite (highlighted by the rectangular frame) corresponds to {1 1 1}-planes of fcc-Al. In addition to Al, long-time annealing induces the crystallization of the equilibrium ternary intermetallic AlYFe phase which usually occurs at temperatures higher than 320 °C, as confirmed by DSC (Fig. 2a) and XRD measurements. The small nanocrystal size clearly indicates that unlike in as-spun samples, thermally activated crystal growth at rather low temperature occurs only slightly in samples previously subjected to large strains. The resulting microstructure is remarkable in terms of its thermal stability against the crystallization reactions. It also highlights the possibility to control the microstructure at the nanometer scale by applying a combination of non-equilibrium processes that may not be obtainable by strain-free methods alone.

5. Conclusion

The analyses of deformation-induced nanocrystallization confirm that nanocrystals develop predominantly within the shear-bands. The deformation might also affect the amorphous phase promoting further crystallization in the amorphous matrix that could account for the remarkably homogeneous nanostructure produced by SPD. Unlike other non-equilibrium processes, the deformation at large strains give also the possibility for controlling the microstructure of marginally glass-forming alloys in bulk shape. For instance, SPD-processing and subsequent isothermal treatments at low temperatures might allow to produce massive nanocrystalline materials with attractive properties.

Acknowledgement

The authors gratefully thank Mr. T. Scherer for the TEM sample preparation.

References

[1] H. Chen, Y. He, G.J. Shiflet, S.C. Poon, Scr. Metall. Mater. 25 (1991) 1421–1424.
[2] R.I. Wu, G. Wilde, J.H. Perepezko, Mater. Sci. Eng. A 301 (2001) 12–17.
[3] H. Chen, Y. He, G.J. Shiflet, S.J. Poon, Nature 367 (1994) 541–543.
[4] W.H. Jiang, M. Atzmon, Acta Mater. 51 (2003) 4095–4105.
[5] Y. He, G.J. Shiflet, S.J. Poon, Acta Metall. Mater. 43 (1995) 83–91.
[6] J.-J. Kim, Y. Choi, S. Suresh, A.S. Argon, Science 295 (2002) 654–657.
[7] R.J. Hebert, N. Boucharat, J.H. Perepezko, H. Rösner, G. Wilde, Proceedings of Metallurgical and Materials Transactions A, in press.
[8] N. Boucharat, R. Hebert, H. Rösner, R. Valiev, G. Wilde, Scr. Mater. 53 (2005) 823–828.
[9] A.S. Argon, Acta Met. 27 (1979) 47.
[10] N. Boucharat, H. Rösner, J.H. Perepezko, G. Wilde, Mater. Sci. Eng. A 375–377 (2004) 713–717.
[11] R.J. Hebert, J.H. Perepezko, Mater. Sci. Eng. A 375–377 (2004) 728–732.